

Parameter Redundancy in the Unitary Coupled-Cluster Ansatz for Hybrid Variational Quantum Computing

Shashank G Mehendale,^{1, a)} Bo Peng,^{2, b)} Niranjana Govind,^{2, c)} and Yuri Alexeev^{3, d)}

¹⁾*Indian Institute of Science Education and Research (IISER), Kolkata, West Bengal 741246, India*

²⁾*Physical and Computational Sciences Directorate, Pacific Northwest National Laboratory, Richland, WA 99354, United States*

³⁾*Computational Science Division, Argonne National Laboratory, Lemont, IL 60439, United States*

(Dated: January 25, 2023)

One of the commonly used chemical-inspired approaches in variational quantum computing is the unitary coupled-cluster (UCC) ansatz. Despite being a systematic way of approaching the exact limit, the number of parameters in the standard UCC ansatz exhibits unfavorable scaling with respect to the system size, hindering its practical use on near-term quantum devices. Efforts have been taken to propose some variants of UCC ansatz with better scaling. In this paper we explore the parameter redundancy in the preparation of unitary coupled-cluster singles and doubles (UCCSD) ansatz employing spin-adapted formulation, small amplitude filtration, and entropy-based orbital selection approaches. Numerical results of using our approach on some small molecules have exhibited a significant cost reduction in the number of parameters to be optimized and in the time to convergence compared with conventional UCCSD-VQE simulations. We also discuss the potential application of some machine learning techniques in further exploring the parameter redundancy, providing a possible direction for future studies.

I. INTRODUCTION

The variational quantum eigensolver (VQE) has arguably emerged as one of the most promising algorithms for the ground state estimation of molecular Hamiltonians in the noisy intermediate-scale quantum (NISQ) era. VQE starts with a given Hamiltonian and a parameterized ansatz state. The expectation value of the Hamiltonian with respect to the ansatz is taken to be the cost function that is minimized by varying the parameters of the ansatz. The task assigned to the quantum computer is to estimate the expectation value, while the task assigned to the classical computer is to predict the new parameter values based on the old expectation value. In this sense, they together form the minimization routine and hence form a quantum-classical hybrid algorithm appropriate for the NISQ era.

The first VQE experiment by Peruzzo and co-workers¹ utilized the unitary coupled-cluster singles and doubles (UCCSD) ansatz derived from unitary coupled-cluster theory^{2–10}. The standard UCCSD ansatz has an unfavorable scaling of the number of parameters with respect to the system size¹¹, which translates to a large number of quantum gates and a long circuit in the quantum simulations. The errors in these quantum gates and circuits can quickly accumulate in the simulation, hindering the practical use of the UCCSD ansatz for simulating large quantum systems on near-term quantum devices.

To prepare ansatz with favorable scaling, researchers have proposed many approaches (see Refs. 12,13 for recent reviews). Usually, the ansatz are classified into hardware-efficient type and chemical-inspired type with either fixed or adaptive structures. Hardware-efficient ansatz are flexi-

ble and easy to implement with the current quantum hardware^{14,15} but suffer from so-called barren plateaus in the variational parameter landscape¹⁶ and require extra work to enforce the physical symmetries. The chemical-inspired ansatz, on the other hand, are usually focused on some UCC variants with improved scaling. Typical UCC variants with fixed circuit structures include the unitary pair coupled cluster with generalized singles and doubles (k -UpCCGSD) method¹⁷ that provides “linear” scaling with the system size while including an unknown prefactor k that needs to be determined heuristically, the orbital-optimized unitary coupled-cluster (OO-UCC) ansatz¹⁸ introducing Brueckner-type orbitals with slight performance improvement, and the double unitary coupled-cluster (DUCC) ansatz^{19,20} naturally enabling the support for more realistic active space approximations.

Between the chemical-inspired and hardware-efficient ansatz there also exists the so-called qubit coupled-cluster (QCC) method introduced by Ryabinkin et al.²¹ resembling the coupled-cluster structure but working directly with Pauli strings in the qubit space to reduce the number of two-qubit gates and pursue the efficient use of quantum resources. In practice, however, since the number of Pauli string candidates for the QCC ansatz have an exponential scaling ($\mathcal{O}(4_q^N)$, with N_q the number of qubits employed), QCC also requires a robust selection process based on an efficient estimate of the contribution of the corresponding entanglers of these Pauli strings to the correlation energy. Regarding chemical-inspired ansatz with adaptive circuit structures, typical developments include the adaptive derivative-assembled pseudo-Trotter ansatz variational quantum eigensolver (ADAPT-VQE)²², the qubit-excitation-based adaptive VQE (QEB-ADAPT-VQE)²³, the iterative QCC approach²⁴, the unitary selective coupled-cluster approach²⁵, sparse UCC ansatz²⁶, and their extensions. The key idea here is to construct an ansatz that can recover most of the correlation energy with the least number of operators and variational parameters, and the

^{a)}Electronic mail: sgm18ms074@iiserkol.ac.in

^{b)}Electronic mail: peng398@pnnl.gov

^{c)}Electronic mail: niri.govind@pnnl.gov

^{d)}Electronic mail: yuri@anl.gov

importance of the operators is typically measured through the energy gradient with respect to the corresponding variation parameters or simply their associate correlation energy contribution.

In this paper we employ other approaches to explore the interconnections between the parameters in the UCC ansatz that would possibly lead to a performance improvement in the UCC ansatz preparation. In particular, we employ spin adaption, small amplitude filtration, and entropy-based orbital selection techniques in the UCCSD framework to explore parameter redundancy. We also discuss the feasibility of applying machine learning techniques in discovering parameter redundancy. The rest of this paper is organized as follows. In Section II we give an introduction to the theoretical background and numerical methodology. In Section III we present some numerical results and the performance of our proposed UCC-VQE approaches for the quantum simulations of some prototype molecular systems. In Section IV we discuss some possible further improvements in this direction. In Section V we summarize our conclusions and briefly present ideas for future work.

II. THEORY AND METHOD

A. Unitary coupled-cluster variational quantum eigensolver

In the UCC ansatz, the UCC operator is the exponential of the conventional cluster operator minus its Hermitian conjugate. For molecular systems, the cluster operator consists of all the excitation operators from the occupied orbitals to the virtual orbitals, which, when acting on the single reference state, produces a linear combination of all possible excited determinants. In practice, the cluster operator is usually truncated to singles, doubles, or a few more excitations. In this work we mainly use the UCCSD approach. The reference state is usually taken to be the Hartree–Fock state of the molecular system, $|\text{HF}\rangle$. Hence a parametrized UCC ansatz is given by

$$|\psi(\vec{\theta})\rangle = e^{\mathbf{T}(\vec{\theta}) - \mathbf{T}^\dagger(\vec{\theta})} |\text{HF}\rangle, \quad (1)$$

where for a UCCSD ansatz we have

$$\mathbf{T}(\vec{\theta}) = \sum_{i,a} t_i^a(\vec{\theta}) a_a^\dagger a_i + \sum_{i<j,a<b} t_{ij}^{ab}(\vec{\theta}) a_a^\dagger a_b^\dagger a_j a_i, \quad (2)$$

with i, j, \dots being occupied spin orbital indices and a, b, \dots being virtual spin orbital indices. Here t_i^a, t_{ij}^{ab} are the single and double cluster amplitudes. The task of VQE is then to provide the minimum value of the expectation value of the Hamiltonian H with respect to the parameterized state as

$$E = \min_{\vec{\theta}} \langle \psi(\vec{\theta}) | H | \psi(\vec{\theta}) \rangle. \quad (3)$$

B. Spin-adapted unitary coupled cluster

The first parameter simplification method we employ in this work is the well-known technique of spin adaption^{27,28}.

In a typical UCC-VQE minimization, each parameter of the excitation operator is treated as an independent variable. Thus, the resulting state from the minimization need not be an eigenstate of the total spin, S^2 , operator. In many cases, however, we expect the ground state of the Hamiltonian to be an eigenstate of the S^2 operator. Hence, in order to make sure that we do not break the spin-symmetry, some conditions on the excitation operators can be used. These ensure that the cluster operator commutes with the S^2 operator and hence leads to an eigenstate of the total spin. Consequently, the number of independent cluster amplitudes is considerably reduced. In Eq. (2), if we relabel the subscripts of cluster amplitudes to mean occupied/virtual spatial orbitals instead of spin orbitals and specifically mention the flavor of the spin (α, β) besides these indices, then the spin adaption relations of a closed shell electron configuration can be given as

$$t_{i\alpha}^{a\alpha} = t_{i\beta}^{a\beta} \quad (4)$$

$$t_{i\alpha j\alpha}^{a\alpha b\alpha} = t_{i\beta j\beta}^{a\beta b\beta} = t_{i\alpha j\beta}^{a\alpha b\beta} + t_{i\alpha j\beta}^{a\beta b\alpha} \quad (5)$$

$$t_{i\alpha j\beta}^{a\alpha b\beta} = t_{i\beta j\alpha}^{a\beta b\alpha} \quad \& \quad t_{i\alpha j\beta}^{a\beta b\alpha} = t_{i\beta j\alpha}^{a\alpha b\beta}. \quad (6)$$

However, as has been noted in the literature²⁹, this procedure reduces only the number of independent parameters supplied to the classical part of the UCC-VQE routine and does not reduce the number of quantum gates and the circuit depth. We also mention that even though we could implement these restrictions to preserve spin symmetry, in a practical implementation we would have to resort to Trotter decomposition, which might actually induce additional errors and hence break the symmetry if the Trotter error is not well controlled²⁹. We will use the spin-adapted UCCSD or its notation SA-UCCSD interchangeably in this paper.

C. Single orbital entropy

Another important concept used in this work is the single orbital entropy³⁰. The von Neumann entropy of a system that is represented by a density matrix ρ is given by

$$S = -\rho \ln \rho = -\sum_i \lambda_i \ln \lambda_i, \quad (7)$$

where λ_i is the i th eigenvalue of the density matrix. For a pure state, the value of the entropy is zero, while for the maximally mixed state, the value of the entropy is maximum. Calculation of entropy is useful for evaluating the amount of entanglement in a system, and it is done by measuring what is known as the entanglement entropy. Given a pure state of a system with two subsystems A and B , the entanglement entropy is defined as the von Neumann entropy of the reduced density matrices of either of the subsystems.

Writing the electronic ground state as a density matrix, we can take any of the molecular orbitals as a single subsystem and the remaining orbitals as another subsystem and calculate the entanglement entropy of this molecular orbital. This calculation gives the amount of entanglement shared between the single molecular orbital and the rest of the molecular orbitals. This entropy for each of the orbitals

is called the single-orbital entropy. Mathematically, let $|\psi\rangle$ be the ground state of the Hamiltonian in the Fock space

$$|\psi\rangle = \sum_{n_1, n_2, \dots} N_{n_1, n_2, \dots} |n_1, n_2, \dots\rangle, \quad (8)$$

where n_i corresponds to the occupation of the i th spatial orbital. That is, n_i can take one value from the set $\{-, \uparrow, \downarrow, \uparrow\downarrow\}$ corresponding to a possible occupation state: no electron, only α electron, only β electron, and both α and β electrons, respectively. The corresponding density matrix will be

$$\rho = \sum_{\substack{n_1, n_2, \dots \\ n'_1, n'_2, \dots}} N_{n_1, n_2, \dots} |n_1, n_2, \dots\rangle \langle n'_1, n'_2, \dots| N^*_{n'_1, n'_2, \dots} \quad (9)$$

Then, for example, the reduced density matrix of the first spatial orbital can be calculated as

$$\rho_1 = \sum_{\substack{n''_2, n''_3, \dots \\ n'_1, n'_2, \dots}} \sum_{\substack{n_1, n_2, \dots \\ n'_1, n'_2, \dots}} N_{n_1, n_2, \dots} \langle n''_2, n''_3, \dots | n_1, n_2, \dots \rangle \times \langle n'_1, n'_2, \dots | n'_2, n'_3, \dots \rangle N^*_{n'_1, n'_2, \dots} \quad (10)$$

Given that both n_1 and n'_1 can take four different values, ρ_1 will be a 4×4 matrix. From this, we can calculate the entanglement entropy or single-orbital entropy of the first spatial orbital as

$$S_1 = -\rho_1 \ln \rho_1 = -\sum_{i=1}^4 \lambda_i \ln \lambda_i, \quad (11)$$

where λ_i is the i th eigenvalue of the reduced density matrix ρ_1 . The value of S_1 is a measure of entanglement between the first spatial orbital and the rest of the orbitals. For example, it is zero when the first orbital can be separated from all the others in Eq. (8). Single-orbital entropy and/or the mutual information are usually employed as a diagnostic measure of the correlation for the active space selection in the complete active space calculations or system partitioning in the quantum embedding calculations^{31–33}. In this work we propose a way to utilize the single-orbital entropy values to conduct orbital selection for correlation energy calculation.

D. Numerical approach

Our proposed UCC-VQE numerical approach consists of three parts: spin adaption, small amplitude filtration, and entropy-based orbital selection. The aim is to minimize the computational cost of the conventional UCC-VQE simulation through exploring and removing the redundancy in the parameter space of the UCC ansatz. Spin adaption was briefly introduced above. The details of the other two techniques used in our algorithm are explained below.

If a certain portion of the parameters stays negligibly small throughout the minimization procedure, then the corresponding excitations can be heuristically identified from the first κ (κ is a small integer and $\kappa_{\min} = 2$) iterations of the UCC-VQE approach and removed afterward. We

denote this approach as small amplitude filtration (SAF). We combine this technique with spin adaption in the UCC-VQE approach to have a more efficient UCC-VQE variant (denoted SA-SAF-UCC-VQE). The SA-SAF-UCC-VQE procedure can be described as follows.

1. Perform conventional UCC-VQE for κ iterations.
2. Apply two conditions on the parameters obtained from the $(\kappa - 1)$ th and κ th iterations: (1) the absolute values of the parameters at the κ th iteration, $|\bar{\theta}|$, need to be smaller than a small cutoff ϵ_1 and (2) the absolute value of the change in the parameter values from the $(\kappa - 1)$ th to the κ th iteration, $|\Delta\bar{\theta}|$, needs to be smaller than another small cutoff ϵ_2 .
3. Drop the parameters that satisfy conditions (1) and (2), and keep optimizing the remaining parameters.

The resulting reduction in the number of parameters and execution time is observed to be significant, as will be shown in Section III, which not only improves the classical part of the VQE algorithm but also reduces the circuit depth on the quantum computer.

Regarding the entropy-based orbital selection, we want to screen out the orbitals that have a significantly lower entropy value, and correspondingly negligible contributions to the total correlation, in comparison with other orbitals. The efficiency of the UCC-VQE simulation can then be improved by freezing these orbitals in the Hamiltonian to obtain an approximate yet sufficiently accurate correlation energy for the whole system. Since the orbital selection is based on the ordering of the orbital entropy values and their relative discrepancy, the approximate reduced density matrices obtained from some low-level correlation approaches can be sufficient for the entropy calculations. In this sense, without explicitly mentioning it, the reduced density matrices are computed at the Møller–Plesset (MP2) level in the present study.

III. NUMERICAL RESULTS

We applied the SA-SAF-UCCSD-VQE approach for computing the ground state energies of five molecular systems— H_4 (Linear), H_4 (Ring), H_6 , LiH, and H_2O —in the STO-3G basis. We used the Qiskit³⁴ module in Python to implement our proposed approach. The *aer_simulator_statevector* backend was used to perform the quantum computing emulation.

We will first explain the structures of the molecules considered. Next, we will show the robustness of the SAF by comparing the number of free parameters in the excitation operator and the time to convergence in the UCCSD-VQE ground state simulations of the five molecules with and without employing spin adaption and/or small amplitude filtration. Then, we will show the accuracy of the algorithm by comparing the converged energy for each of the three algorithms presented here. After that, we will discuss the improvement offered by the entropy calculations.

For each of the molecules discussed below, unless mentioned otherwise, the SciPy³⁵ minimizer *L-BFGS-B* has

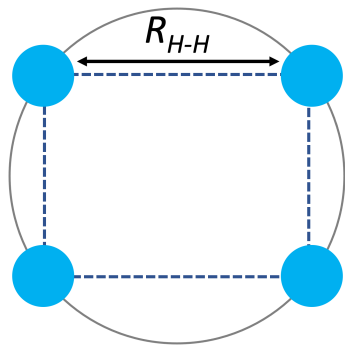


Figure 1. H_4 on a ring.

been used for the classical minimization routine that constitutes the classical part of the UCC-VQE algorithm. The initial parameter values for all the amplitudes of the ansatz have been chosen to be zero. The Hartree–Fock state has been used as the reference for the ansatz. The Jordan–Wigner³⁶ transformation is employed to convert Fermionic operators to Pauli operators.

A. Molecular Structures

- The molecule H_4 consists of 4 electrons and 8 spin orbitals in the STO-3G basis and can be considered in different spatial structures. In this work we focus mainly on two structures, the linear and the ring. In the linear structure, all the hydrogen atoms are present on the same axis, and we have taken the bond length between every adjacent hydrogen atom to be the same. For the ring structure of the H_4 molecule, we consider the four hydrogen atoms forming a rectangle with the vertices to be on a ring, as depicted in Fig. 1.
- We have considered only the linear structure of the H_6 molecule for this work. Here all the hydrogen atoms are present on the same axis, and we have taken the distance between adjacent hydrogen atoms to be the same. We vary the H-H bond length from 0.5 Å to 3.2 Å. H_6 consists of 6 electrons and 12 spin orbitals in the STO-3G basis.
- The geometry of the LiH molecule is simple, comprising just two atoms. The bond length has been varied from 0.8 Å to 4 Å. LiH has 4 electrons and 8 spin orbitals in the STO-3G basis.
- H_2O is a planar molecule with the H-O-H bond making an angle of 104.5° . We have taken O-H bond distances from 0.65 Å to 1.70 Å. The molecule consists of 10 electrons in 14 spin orbitals in the STO-3G basis.

B. Performance of SA-SAF-UCCSD-VQE

To understand the improvement offered by spin adaption and small amplitude filtration, we first look at the number of free parameters reduced by employing these schemes in the UCCSD-VQE approach and the time to convergence in the ground state simulations of the five molecules. We collected the number of free parameters required in three approaches UCCSD-VQE, SA-UCCSD-VQE, and SA-SAF-UCCSD-VQE. The comparison is given in Fig. 2a. As can be seen, compared with the conventional UCCSD-VQE, spin adaption in SA-UCCSD-VQE can reduce the number of parameters in the optimization by roughly half; and combining both spin adaption and small amplitude filtration as in SA-SAF-UCCSD-VQE further reduces the number of free parameters to be only roughly one-quarter of that in the conventional UCCSD-VQE. Since the number of parameters that need to be optimized is greatly reduced, the VQE execution time is also significantly reduced. As shown in Fig. 2b, as the system size grows and bond length elongates (the latter usually indicates the electron correlation gets stronger), the time saved by combining spin adaption and small amplitude filtration is more significant than that by employing only spin adaption in the UCCSD-VQE approach. A typical example can be observed in the VQE quantum simulations of H_2O at $O-H=1.4$ Å, where the execution time of SA-UCCSD-VQE is almost the same as that of UCCSD-VQE, while SA-SAF-UCCSD-VQE reduces the execution time by almost an order of magnitude. We mention that in the SA-SAF-UCCSD-VQE simulations, we set $\kappa = \kappa_{\min} = 2$. Figure 3 shows the average values of the amplitudes (identified as the small amplitudes after $\kappa = 2$ UCCSD-VQE iterations) at the end of the UCCSD-VQE simulations of the five molecules at different bond lengths. As can be seen, the average values of the small amplitudes at the end of the UCCSD-VQE simulations remain mostly less than 10^{-5} throughout the bond length range, indicating that their changes and impact on the minimization are trivial.

We further compare the potential energy surfaces (PES’s) computed by different UCCSD-VQE noise-free simulations discussed here, as well as by the exact diagonalization. The results are shown in Fig. 4. As can be seen, all the PES’s obtained from the UCCSD-VQE noise-free simulations agree with the ideal PES’s very well, and the differences are well below the chemical accuracy ($\sim 1.6 \times 10^{-3}$ Hartree). Looking more closely at the extent of overlap, we see that the second column of Fig. 4 shows the error between the UCCSD-VQE energies and the SA-UCCSD-VQE energies, and the third column shows the error between the SA-UCCSD-VQE energies and SA-SAF-UCCSD-VQE energies. We can clearly see that all the errors are extremely small (with the highest being on the order of 10^{-5} for H_2O), proving that removing the small amplitudes makes a negligible difference in the converged energies as compared with the approach that retains these amplitudes, and the small amplitude filtering is reliable for calculating the ground states of the studied molecules. We mention that the small amplitude filtering approach is completely independent of spin adaption and hence a general scheme that can be ap-

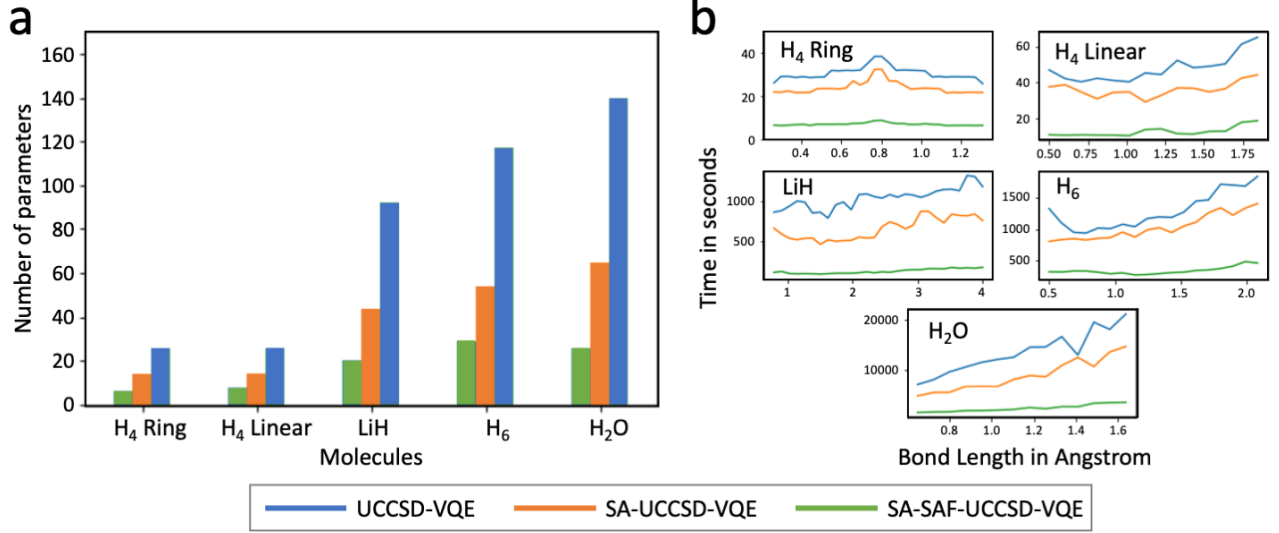


Figure 2. Performance of the UCCSD-VQE (blue), SA-UCCSD-VQE (orange), and SA-SAF-UCCSD-VQE (green) approaches for obtaining the ground states of five molecules in terms of (a) the number of the parameters and (b) the time to convergence. In the SA-SAF-UCCSD-VQE approach, we set $\kappa = 2$, $\epsilon_1 = 10^{-4}$, and $\epsilon_2 = 10^{-5}$. In all the UCCSD-VQE calculations, the convergence is reached when the energy variant is less than 10^{-6} a.u.

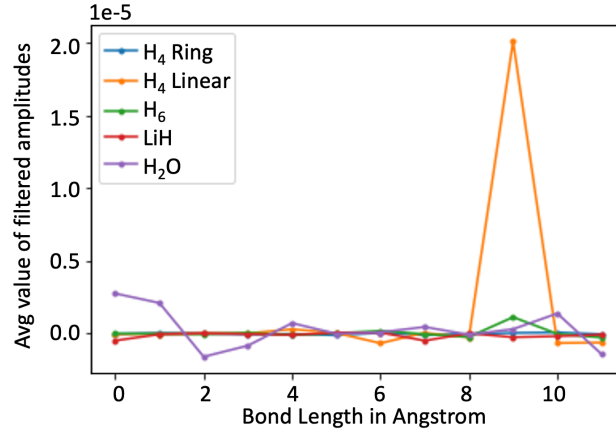


Figure 3. Average values of the small amplitudes at the end of UCCSD-VQE simulations of the five molecules at different bond lengths. Each molecule is scanned over a range of bond lengths that have been discretized to 12 bond length indices.

plied to any UCC-VQE approach at any stage.

Note that in these simulations we did not take symmetry into account. If symmetry is taken into account, the classical minimization procedure can be further improved. Take LiH computed at HF/STO-3G as an example. The excitations including its SA-SAF-UCCSD ansatz are

$$\left\{ \tau_{0,}^2, \tau_{0,}^5, \tau_{1,}^2, \tau_{1,}^5, \tau_{0,1}^{2,5}, \tau_{0,7}^{2,11}, \tau_{0,7}^{2,8}, \tau_{0,7}^{3,9}, \tau_{0,7}^{4,10}, \tau_{0,7}^{5,11}, \tau_{0,6}^{2,11}, \tau_{1,7}^{2,11}, \tau_{0,6}^{2,8}, \tau_{0,6}^{3,9}, \tau_{0,6}^{4,10}, \tau_{0,6}^{5,11}, \tau_{1,7}^{2,8}, \tau_{1,7}^{3,9}, \tau_{1,7}^{4,10}, \tau_{1,7}^{5,11} \right\}, \quad (12)$$

where the orbital indices #0–#5 correspond to α spin orbitals with #0 and #1 occupied and others unoccupied and the indices #6–#11 correspond to β spin orbitals with #6 and #7 occupied and others unoccupied. Since the unoccupied π orbitals #3, #4, #9, and #10 are degenerate, the two sets $\left\{ \tau_{0,7}^{3,9}, \tau_{0,6}^{3,9}, \tau_{1,7}^{3,9} \right\}$ and $\left\{ \tau_{0,7}^{4,10}, \tau_{0,6}^{4,10}, \tau_{1,7}^{4,10} \right\}$ become interchangeable, and only one set needs to be optimized in

the minimization procedure. Note that this treatment does not help reduce the load on the quantum computer since all the operators in (12) still need to be implemented on the quantum side to form the UCCSD ansatz.

C. Improvement through orbital selection

Selecting a portion of the orbitals in the UCC-VQE calculations while still maintaining the accuracy at a desired level not only reduces the number of free parameters but also reduces the number of qubits required to encode the problem on a quantum computer. In this section we use the H₂O molecule as an example to demonstrate the potential improvement in the computational efficiency brought by the entropy-based orbital selection. The computed single-orbital entropies of the H₂O molecule over the studied O–H bond length are shown in Fig. 5a, from which several

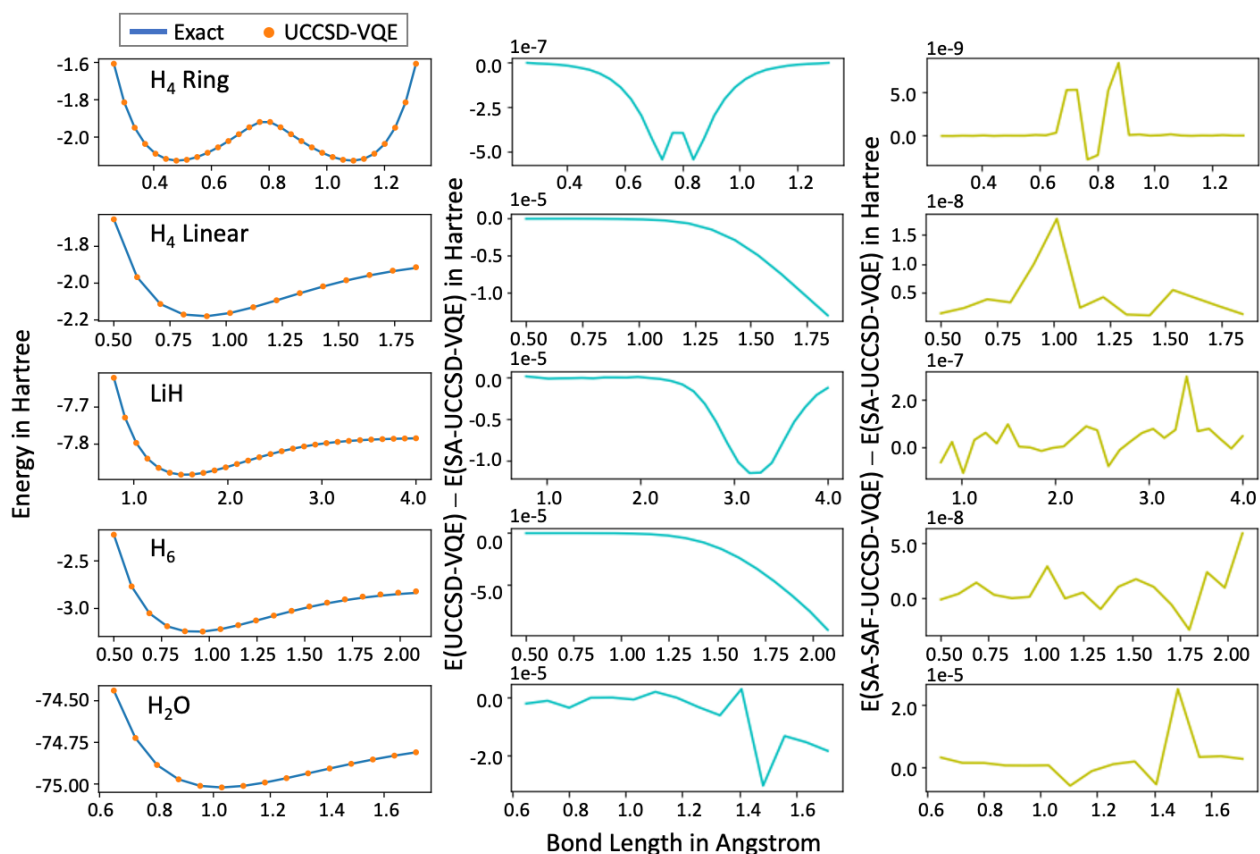


Figure 4. Potential energy surfaces of the five molecules computed by three UCCSD-VQE approaches. Left: the PES computed by conventional UCCSD-VQE and exact diagonalization. Middle: the difference between the SA-UCCSD-VQE energies and the UCCSD-VQE energies for all five molecules at different bond lengths. Right: the difference between the SA-SAF-UCCSD-VQE energies and the SA-UCCSD-VQE energies for all five molecules at different bond lengths.

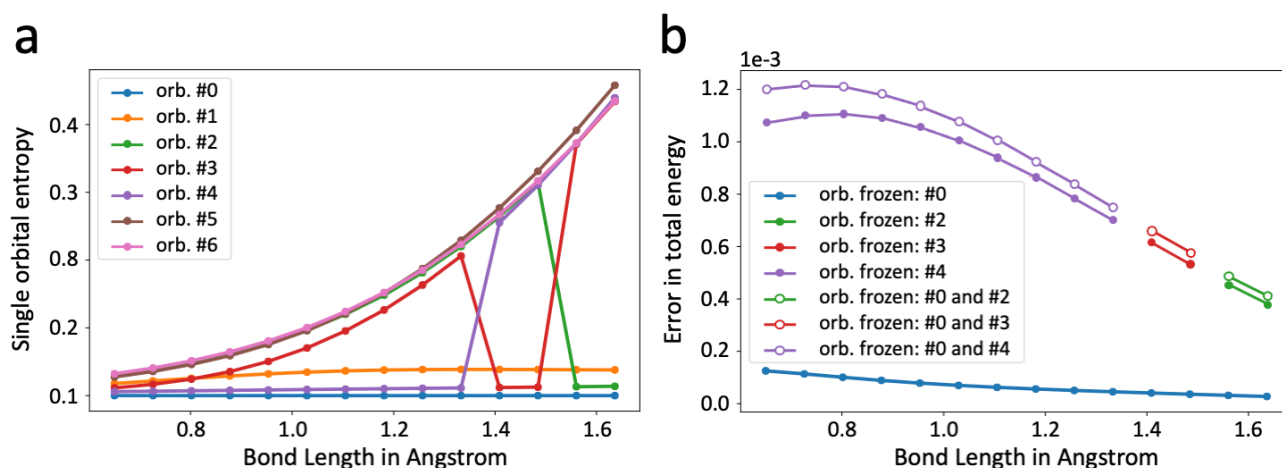


Figure 5. (a) Single orbital entropies of the H_2O molecule computed at the MP2/STO-3G level. (b) Error in energy induced by freezing the different orbitals.

observations can be made.

- The entropies of orbitals #0 and #1 do not exhibit significant change over the entire bond length range. In particular, the entropies of orbital #0 are sufficiently small ($\sim 10^{-5}$) in comparison with the entropies of other orbitals (≥ 0.01).

- Regardless of the bond length, the entropies of orbitals #5 and #6 are always the largest in comparison with the entropies of other orbitals, and they keep increasing with the increasing bond length. Therefore, the entropy discrepancy (for example, between orbitals #5 (or #6) and #0) becomes larger with the increasing bond length.

- The entropy ordering of orbitals #2, #3, and #4 does not stay the same over the studied bond length range. Although the ordering exhibits crossovers over the entire bond length range, the smallest one is very close to the entropy of orbital #0 (the discrepancy is < 0.01).

From these observations, since orbitals #0 and #2/#3/#4 become less important in contributing to the total correlation, they can be frozen from the original Hamiltonian. Specifically, (i) if the bond length $< 1.4 \text{ \AA}$, orbitals #0 and/or #4 can be frozen, (ii) if the bond length is between 1.4 \AA and 1.5 \AA , orbitals #0 and/or #3 can be frozen, and (iii) if the bond length $> 1.5 \text{ \AA}$, orbitals #0 and/or #2 can be frozen. Figure 5b compares the ground state energy of the Hamiltonian with and without freezing these orbitals through exact diagonalization. As can be seen, the error brought by freezing these orbitals is well below the chemical accuracy ($\sim 1.6 \times 10^{-3}$ a.u.), and the error gets smaller with the increasing bond length. In terms of improving the UCC-VQE efficiency, for the studied H_2O molecule, by removing one or two occupied orbitals, we reduce the number of qubits required from 14 to 12 or 10, respectively, and at the same time reduce the number of parameters in the UCCSD ansatz from 140 to 92 or 54, respectively.

IV. DISCUSSION

While the results described above demonstrate the efficiency of the approach proposed in this work, we are considering further improvement. For example, in the case of SA-SAF-UCCSD-VQE, the cutoffs, ϵ_1 , and ϵ_2 , and the heuristic number of iterations, κ , can be tweaked to balance the efficiency and accuracy.

We can further speed up our approach by analyzing the relationship between the excitation parameters. For example, in Eq. (5), to implement spin adaption for the closed-shell electronic configuration, we have three choices: we can take any two of the three excitation coefficients to be independent and write the third one as a function of the remaining two. In such a situation, if we apply small amplitude filtration after a spin adaption, the third parameter could be filtered out while the remaining two parameters, despite being close to each other, are minimized as independent parameters. Thus, we can perform small amplitude filtration before applying spin adaption. If the filtered parameters turn out to be one of the three quantities in Eq. (5), then only one of the remaining two could be explicitly included in the minimizer.

A more involved theoretical analysis could also be done to further reveal the connection between the parameters. Possible ways including employing the mutual information³⁷⁻³⁹ or evaluating the entropy of the wavefunction using the determinant amplitudes²⁶. For example, besides calculating the single-orbital entropies, we could also calculate two-orbital entropies from a 16×16 two-body reduced density matrix, where the trace would be taken over by all except two orbitals. Then, the mutual information could be

calculated through

$$I_{i,j} = \frac{1}{2}(S_i + S_j - S_{ij}).$$

The value of the mutual information could be used in predicting possible dependencies among the parameters. A similar idea has been employed in the ADAPT-VQE algorithm⁴⁰ and could also be used for exploring the interconnection between the excitation operators involving more than two spatial orbitals.

Furthermore, one might anticipate the existence of other hidden relations among the remaining parameters. A way to explore such hidden relations has been reported recently (see Refs. 41,42), where it has been observed through phase analysis that the coupled-cluster amplitudes could be divided into principal and auxiliary categories and that a synergistic relationship between them exists during the iteration dynamics. To find such a classification as well as the synergistic relationship, one could rely on some machine learning (ML) techniques. Here, as an exploratory attempt, we have prototyped an ML-assisted UCC-VQE approach, whose procedure can be summarized as follows.

1. Perform the UCC-VQE calculation for n iterations.
2. Build a regression model based on the existing data obtained from step 1:
 - (a) Label the parameters in the n^{th} UCC-VQE iteration into principal and auxiliary amplitudes according to a predefined absolute value cutoff ϵ .
 - (b) Using the labels in step 1 to collect the principal and auxiliary parameters from n iterations to form the subsets \mathbf{X} and \mathbf{Y} , respectively.
 - (c) Treat subset \mathbf{X} as a set of independent variables and subset \mathbf{Y} as a set of dependent variables, and solve the regression problem $\mathcal{F} : \mathbf{X} \rightarrow \mathbf{Y}$.
3. Once the regression function is developed, proceed to new iterations, where only the new principal amplitudes are evaluated. The new auxiliary amplitudes are generated by applying the regression function to the new principal amplitudes.
4. Once the minimizer in step 3 reaches convergence, the resulting amplitudes will be taken out and supplied back to the UCC operator of step 1 to perform another n UCC-VQE iterations.
5. Repeat steps 2 to 4 until convergence is reached. The convergence is marked by one of two scenarios: either the UCC-VQE simulation in step 1 terminates within n iterations, or step 4 reaches convergence in a single iteration.

If one is considering a linear regression model, then the regression model will be given by

$$\mathbf{Y} = \mathcal{F}(\mathbf{X}) = \mathbf{X} \cdot \boldsymbol{\beta}, \quad (13)$$

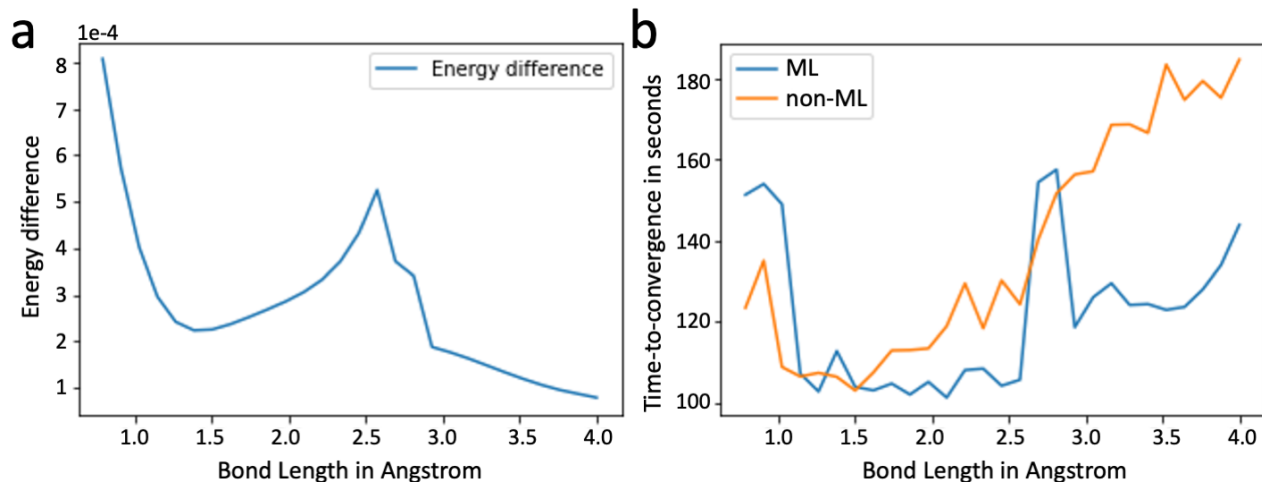


Figure 6. Efficiency of the ML-assisted SA-SAF-UCCSD-VQE simulations for the LiH molecule at different bond lengths in terms of (a) the energy difference and (b) the time-to-convergence in comparison with the non-ML SA-SAF-UCCSD-VQE simulations. In the ML-assisted simulations at each bond length, $\sim 30\%$ – 40% of the total amplitudes from $n = 4$ SA-SAF-UCCSD-VQE iterations are taken to be the principal amplitudes to construct a nonlinear regression model employing Eq. (17) as the kernel with $\gamma = 1$, $c_0 = 0$, and $d = 3$.

and the “slope” β can be obtained by minimizing the cost function

$$\mathcal{C} = \|\mathbf{Y} - \mathcal{F}(\mathbf{X})\|_F^2 + \lambda \mathcal{R}(\beta) \quad (14)$$

through

$$\frac{\partial \mathcal{C}}{\partial \beta} = 0 \Rightarrow \beta = \mathbf{X}^T (\mathbf{X}\mathbf{X}^T + \lambda \mathbf{I})^{-1} \mathbf{Y}. \quad (15)$$

Here the subscript F denotes the Frobenius norm, and $\mathcal{R}(\beta)$ is a slope-dependent ridge term, which is added to enhance the robustness of the regression function on the test data. In the practical implementation, since the combination of Eqs. (13) and (15) includes only the so-called kernel term

$$\mathcal{K} = \mathbf{X}\mathbf{X}^T, \quad (16)$$

there is no need to explicitly compute β . To build a more general non-linear regression model, one can replace the kernel term by, for example, its polynomial form

$$\mathcal{K}(x_i, x_j) = (\gamma x_i x_j^T + c_0)^d, \quad (17)$$

where x_i is the i^{th} row vector of subset X , d is the order of the polynomial, and γ and c_0 are free parameters.

We have performed the ML-assisted SA-SAF-UCCSD-VQE simulation for the LiH molecule. The energy differences and the time to convergence compared with the non-ML SA-SAF-UCCSD-VQE simulations are given in Fig. 6. As can be seen, the energy differences between the ML and non-ML versions of the SA-SAF-UCCSD-VQE simulations are mostly on the order of 10^{-4} at most of the bond lengths. The time to convergence between the two versions at smaller bond lengths is comparable, but the ML-assisted simulation is clearly less time-consuming than the non-ML version at larger bond lengths (i.e., stronger correlation). We note that here we have explored a polynomial dependence of the auxiliary amplitudes on the principal

ones in a heuristic manner. Other types of kernel functions could also be tested. Generally speaking, a kernel function that is more physically motivated would predict the relationship among the parameters more accurately.

V. CONCLUSION

In this work we have shown that the conventional UCC-VQE calculations can be improved significantly even after considering the spin adaption technique. The corresponding noise-free UCC-VQE simulations of some small molecules at various bond lengths show that a significant portion of cluster amplitudes are sufficiently small throughout the simulations, and these amplitudes can be identified heuristically from the first few UCC-VQE iterations. Thus, eliminating these amplitudes improves both quantum and classical calculations. Next, we proposed a way to freeze molecular orbitals based on their single-orbital entropy values calculated from a low-level theory such as MP2. Using the H_2O molecule as an example, we demonstrated that freezing the orbitals that have low enough entropy values compared with the rest can further simplify the ansatz with well-controlled error in energy. Furthermore, we explored the feasibility of employing some ML techniques for identifying other possible hidden relationships between the amplitudes. This work opens up some possible future directions. For example, one direction is how to build a more appropriate, physically motivated kernel that, when combined with the right pair of principal and auxiliary amplitude subsets, would give a better result. Although here we have used a single kernel, the entire amplitude set could be divided into multiple principal and auxiliary amplitude subsets with a unique kernel for each pair of subsets, which might be able to further improve the UCC-VQE simulations.

ACKNOWLEDGMENT

This material is based upon work supported by the U.S. Department of Energy, Office of Science, and National Quantum Information Science Research Centers. Y.A. acknowledges support from the U.S. Department of Energy, Office of Science, under contract DE-AC02-06CH11357 at Argonne National Laboratory.

REFERENCES

- ¹Alberto Peruzzo, Jarrod McClean, Peter Shadbolt, Man-Hong Yung, Xiao-Qi Zhou, Peter J. Love, Alán Aspuru-Guzik, and Jeremy L. O’Brien. A variational eigenvalue solver on a photonic quantum processor. *Nat. Commun.*, 5(1):4213, 2014.
- ²Sourav Pal. Use of a unitary wavefunction in the calculation of static electronic properties. *Theor. Chim. Acta*, 66(3-4):207–215, 1984.
- ³Chiranjib Sur, Rajat K Chaudhuri, Bijaya K Sahoo, BP Das, and D Mukherjee. Relativistic unitary coupled cluster theory and applications. *J. Phys. B*, 41(6):065001, 2008.
- ⁴Bridgette Cooper and Peter J Knowles. Benchmark studies of variational, unitary and extended coupled cluster methods. *J. Chem. Phys.*, 133(23):234102, 2010.
- ⁵Rodney J. Bartlett, Stanislaw A. Kucharski, and Jozef Noga. Alternative coupled-cluster ansätze II. the unitary coupled-cluster method. *Chem. Phys. Lett.*, 155(1):133–140, 1989.
- ⁶Andrew G Taube and Rodney J Bartlett. New perspectives on unitary coupled-cluster theory. *Int. J. Quantum Chem.*, 106(15):3393–3401, 2006.
- ⁷Mark R Hoffmann and Jack Simons. A unitary multiconfigurational coupled-cluster method: Theory and applications. *J. Chem. Phys.*, 88(2):993–1002, 1988.
- ⁸Werner Kutzelnigg. Error analysis and improvements of coupled-cluster theory. *Theor. Chim. Acta*, 80(4-5):349–386, 1991.
- ⁹Francesco A Evangelista, Garnet Kin-Lic Chan, and Gustavo E Scuseria. Exact parameterization of fermionic wave functions via unitary coupled cluster theory. *J. Chem. Phys.*, 151(24):244112, 2019.
- ¹⁰Abhinav Anand, Philipp Schleich, Sumner Alperin-Lea, Phillip WK Jensen, Sukin Sim, Manuel Díaz-Tinoco, Jakob S Kottmann, Matthias Degroote, Artur F Izmaylov, and Alán Aspuru-Guzik. A quantum computing view on unitary coupled cluster theory. *Chem. Soc. Rev.*, 2022.
- ¹¹Michael Kühn, Sebastian Zanker, Peter Deglmann, Michael Marthaler, and Horst Weiß. Accuracy and resource estimations for quantum chemistry on a near-term quantum computer. *J. Chem. Theory Comput.*, 15(9):4764–4780, 2019.
- ¹²D.A. Fedorov, B. Peng, N. Govind, and Y. Alexeev. VQE method: a short survey and recent developments. *Mater. Theory*, 6:2, 2022.
- ¹³The variational quantum eigensolver: A review of methods and best practices. *Phys. Rep.*, 986:1–128, 2022.
- ¹⁴Abhinav Kandala, Antonio Mezzacapo, Kristan Temme, Maika Takita, Markus Brink, Jerry M. Chow, and Jay M. Gambetta. Hardware-efficient variational quantum eigensolver for small molecules and quantum magnets. *Nature*, 549(7671):242–246, 2017.
- ¹⁵Abhinav Kandala, Kristan Temme, Antonio D. Córcoles, Antonio Mezzacapo, Jerry M. Chow, and Jay M. Gambetta. Error mitigation extends the computational reach of a noisy quantum processor. *Nature*, 567(7749):491–495, 2019.
- ¹⁶Jarrold R. McClean, Sergio Boixo, Vadim N. Smelyanskiy, Ryan Babush, and Hartmut Neven. Barren plateaus in quantum neural network training landscapes. *Nat. Commun.*, 9(1):4812, 2018.
- ¹⁷Joonho Lee, William J Huggins, Martin Head-Gordon, and K Birgitta Whaley. Generalized unitary coupled cluster wave functions for quantum computation. *J. Chem. Theory Comput.*, 15(1):311–324, 2018.
- ¹⁸Wataru Mizukami, Kosuke Mitarai, Yuya O. Nakagawa, Takahiro Yamamoto, Tennin Yan, and Yu-ya Ohnishi. Orbital optimized unitary coupled cluster theory for quantum computer. *Phys. Rev. Research*, 2:033421, Sep 2020.
- ¹⁹Mekena Metcalf, Nicholas P. Bauman, Karol Kowalski, and Wibe A. de Jong. Resource-efficient chemistry on quantum computers with the variational quantum eigensolver and the double unitary coupled-cluster approach. *J. Chem. Theory Comput.*, 16(10):6165–6175, 2020. PMID: 32915568.
- ²⁰Karol Kowalski. Properties of coupled-cluster equations originating in excitation sub-algebras. *J. Chem. Phys.*, 148(9):094104, 2018.
- ²¹Ilya G. Ryabinkin, Tzu-Ching Yen, Scott N. Genin, and Artur F. Izmaylov. Qubit coupled cluster method: A systematic approach to quantum chemistry on a quantum computer. *J. Chem. Theory Comput.*, 14(12):6317–6326, 2018.
- ²²Harper R. Grimsley, Sophia E. Economou, Edwin Barnes, and Nicholas J. Mayhall. An adaptive variational algorithm for exact molecular simulations on a quantum computer. *Nat. Commun.*, 10(1):3007, dec 2019.
- ²³Y. S. Yordanov, V. Armaos, C. H. W. Barnes, and D. R. M. Arvidsson-Shukur. Qubit-excitation-based adaptive variational quantum eigensolver. *Commun. Phys.*, 4:228, 2021.
- ²⁴Ilya G. Ryabinkin, Robert A. Lang, Scott N. Genin, and Artur F. Izmaylov. Iterative qubit coupled cluster approach with efficient screening of generators. *J. Chem. Theory Comput.*, 16(2):1055–1063, 2020.
- ²⁵Dmitry A. Fedorov, Yuri Alexeev, Stephen K. Gray, and Matthew Otten. Unitary selective coupled cluster method. *Quantum*, 6:703, May 2022.
- ²⁶J. Wayne Mullinax and Norm M. Tubman. Large-scale sparse wavefunction circuit simulator for applications with the variational quantum eigensolver, 2023.
- ²⁷Josef Paldus. Correlation problems in atomic and molecular systems, V: Spin-adapted coupled cluster many-electron theory. *J. Chem. Phys.*, 67(1):303–318, 1977.
- ²⁸Gustavo E Scuseria, Andrew C Scheiner, Timothy J Lee, Julia E Rice, and Henry F Schaefer III. The closed-shell coupled cluster single and double excitation (CCSD) model for the description of electron correlation. a comparison with configuration interaction (CISD) results. *J. Chem. Phys.*, 86(5):2881–2890, 1987.
- ²⁹Takashi Tsuchimochi, Yuto Mori, and Seiichiro L. Ten-no. Spin-projection for quantum computation: A low-depth approach to strong correlation. *Phys. Rev. Research*, 2:043142, Oct 2020.
- ³⁰Katharina Boguslawski and Paweł Tecmer. Orbital entanglement in quantum chemistry. *Int. J. Quantum Chem.*, 115(19):1289–1295, 2015.
- ³¹Katharina Boguslawski, Paweł Tecmer, Gergely Barcza, Örs Legeza, and Markus Reiher. Orbital entanglement in bond-formation processes. *J. Chem. Theory Comput.*, 9(7):2959–973, 2013.
- ³²Pavlo Golub, Andrej Antalik, Libor Veis, and Jiri Brabec. Machine learning-assisted selection of active spaces for strongly correlated transition metal systems. *J. Chem. Theory Comput.*, 17(10):6053–6072, 2021.
- ³³Jonathan M. Waldrop, Theresa L. Windus, and Niranjan Govind. Projector-based quantum embedding for molecular systems: An investigation of three partitioning approaches. *J. Phys. Chem. A*, 125(29):6384–6393, 2021.
- ³⁴Qiskit: An open-source framework for quantum computing, 2021.
- ³⁵Pauli Virtanen, Ralf Gommers, Travis E. Oliphant, Matt Haberland, Tyler Reddy, David Cournapeau, Evgeni Burovski, Pearu Peterson, Warren Weckesser, Jonathan Bright, Stéfan J. van der Walt, Matthew Brett, Joshua Wilson, K. Jarrod Millman, Nikolay Mayorov, Andrew R. J. Nelson, Eric Jones, Robert Kern, Eric Larson, C J Carey, İlhan Polat, Yu Feng, Eric W. Moore, Jake VanderPlas, Denis Laxalde, Josef Perktold, Robert Cimrman, Ian Henriksen, E. A. Quintero, Charles R. Harris, Anne M. Archibald, Antônio H. Ribeiro, Fabian Pedregosa, Paul van Mulbregt, and SciPy 1.0 Contributors. SciPy 1.0: Fundamental Algorithms for Scientific Computing in Python. *Nature Methods*, 17:261–272, 2020.
- ³⁶P. Jordan and E. Wigner. Über das paulische Äquivalenzverbot. *Z. Physik*, 47:631–651, 1928.
- ³⁷Luigi Amico, Rosario Fazio, Andreas Osterloh, and Vlatko Vedral. Entanglement in many-body systems. *Rev. Mod. Phys.*, 80:517–576, May 2008.
- ³⁸Jörg Rissler, Reinhard M. Noack, and Steven R. White. Measuring orbital interaction using quantum information theory. *Chem. Phys.*, 323(2):519–531, 2006.
- ³⁹Zhen Huang and Sabre Kais. Entanglement as measure of electron–electron correlation in quantum chemistry calculations. *Chem. Phys. Lett.*, 413(1):1–5, 2005.
- ⁴⁰Zi-Jian Zhang, Thi Ha Kyaw, Jakob S Kottmann, Matthias Degroote, and Alán Aspuru-Guzik. Mutual information-assisted adaptive variational

- quantum eigensolver. *Quantum Sci. Technol.*, 6(3):035001, aug 2021.
- ⁴¹Valay Agarawal, Samrendra Roy, Anish Chakraborty, and Rahul Maitra. Accelerating coupled cluster calculations with nonlinear dynamics and supervised machine learning. *J. Chem. Phys.*, 154(4):044110, 2021.
- ⁴²Valay Agarawal, Samrendra Roy, Kapil K Shrawankar, Mayank Ghogale, S Bharathi, Anchal Yadav, and Rahul Maitra. A hybrid coupled cluster–
machine learning algorithm: Development of various regression models and benchmark applications. *J. Chem. Phys.*, 156(1):014109, 2022.